Article

Contact Angle Hysteresis Generated by Strong Dilute Defects

Mathilde Reyssat, and David Que#re#

J. Phys. Chem. B, **2009**, 113 (12), 3906-3909• DOI: 10.1021/jp8066876 • Publication Date (Web): 11 February 2009

Contact Angle Hysteresis Generated by Strong Dilute Defects†

Mathilde Reyssat and David Quéré*

Physique et Mécanique des Milieux Hétérogènes, UMR 7636 du CNRS, ESPCI, 75005 Paris, France

Received: July 28, 2008; Revised Manuscript Received: November 10, 2008

Water on solid decorated with hydrophobic defects (such as micropillars) often stays at the top of the defects in a so-called fakir state, which explains the superhydrophobicity observed in such case, provided that the density of defects is small enough. Here we show that this situation provides an ideal frame for studying the contact angle hysteresis; the phase below the liquid is "perfect" and slippery (it is air), contrasting with pillars' tops whose edges form strong pining sites for the contact line. This model system thus allows us to study the hysteresis as a function of the density of defects and to compare it to the classical theory by Joanny and de Gennes, which is based on very similar hypothesis.

Introduction

The effect of texture on wettability has been extensively investigated for the last ten years, because textures can bring spectacular original properties, such as superhydrophilicity and superhydrophobicity, making it possible to build water repellent,[1] antifogging,[2] or superslippery[3] materials. Here we focus on hydrophobic solids covered by cylindrical pillars, a simple design for which each parameter (height, mutual distance, and diameter of the pillars) can be varied independently. Controlling these parameters allows us to study quantitatively a given property, such as wettability, slip, or here degree of adhesion of water.[4] Two main states are possible for a water drop deposited on such a material: either the liquid follows the solid surface (Wenzel state),[5] or it stands at the tops of the pillars (Cassie or fakir state) owing to the chemical hydrophobicity.[6] These two states provide highly contrasted water adhesion:[7,8] a Wenzel drop is deeply pinned in the texture, and thus exhibits a giant contact angle hysteresis, which can even exceed 100°! In contrast, fakir drops hardly stick to the substrate, which of course defines the situation of practical interest: these drops are readily evacuated by a slope, air blowing, or any small force acting on them. However, a residual water adhesion is generally observed on these materials.[8,9] It can be determined by either measuring the tilting angle above which a drop of a given volume starts moving[9] or directly measuring the maximum and minimum static angles θ_a and θ_r. Our definition for the contact hysteresis will be $\Delta\cos\theta = \cos\theta_r - \cos\theta_a$; the larger the number $\Delta\cos\theta$ (always between 0 and 2), the larger the adhesion. Here we discuss this quantity, whose expression and calculation are still the subject of very active debates.[10−15] We measure $\Delta\cos\theta$ in the fakir regime on a series of samples where the density ϕ of micropillars is the only variable parameter, and we discuss how the hysteresis increases with ϕ.

Using soft lithography and ion etching,[16] we achieved samples planted with identical cylindrical pillars (radius $b = 1.2$ μm and height $h = 6$ μm) separated by a slowly varying distance p in the range of a few micrometers (Figure 1). Thus, the pillar density ϕ is varied on a "unique" sample. This is a key point; measuring (receding and advancing) contact angles on "different" samples of various pillar densities yields much more scattered data. For different samples, pillar characteristics (diameter, shape of the edges at the pillars' tops, etc.) slightly change, which impacts significantly the value of the angles; in contrast, we work here with samples where the only variable parameter is the pillar density (typically between 5% and 30%), keeping unchanged the pillars' characteristics. The samples are made of silicon and covered with a fluoropolymer, which provides hydrophobicity.[16]

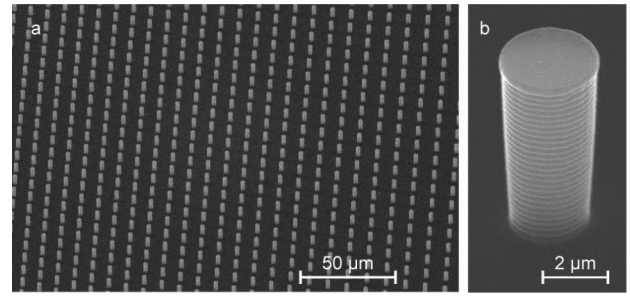

Figure 1. Top view of materials decorated with identical pillars whose density ϕ slowly varies along the centimetric size of the sample. In (a), ϕ varies by 4% per millimeter from 8 to 7% from left to right on a distance of 0.25 mm. In (b), we can see one of the cylindrical pillars of radius $b = 1.2$ μm and height $h = 6$ μm.

Millimeter-size water drops were all observed to be in the fakir state whatever the pillar density, as shown by their mobility when tilting the plate. (Wenzel drops of similar volume would remain pinned, whatever the tilting angle.) Since a fakir contact angle is a function of ϕ (the smaller ϕ, the larger the proportion of air below the drop, and thus the larger the angle), water drops might spontaneously move toward regions of larger ϕ (that is, smaller hydrophobicity). In order to minimize this phenomenon, we worked with a small gradient ($\nabla\phi = 2.3\%$ per millimeter). The drops never self-propel, owing to a non-negligible contact angle hysteresis or equivalently to an anchoring force resisting the weak wettability gradient. The choice of a small $\nabla\phi$ also minimizes the variation of ϕ below the drop, whose base is about two millimeters; the uncertainty on the knowledge of ϕ is thus $\pm 3\%$.

The sample is placed on a rotating table, and a few drops (volume $\Omega = 10$ or 20 μL) are deposited along the same line (perpendicular to the slope, along the gradient of pillar density). As the slope is gradually increased, the drops are successively

† Part of the "PGG (Pierre-Gilles de Gennes) Memorial Issue".

* To whom correspondence should be addressed.

10.1021/jp8066876 CCC: $40.75
Published on Web 02/11/2009

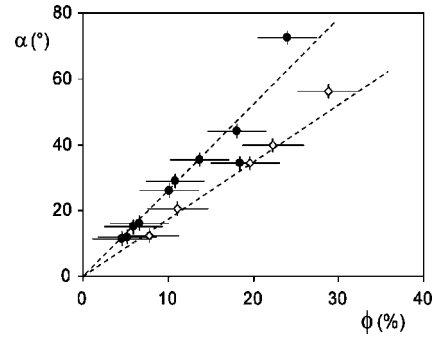

Figure 2. Tilting angle α at which a drop of volume Ω starts moving on a sample decorated with a density ϕ of cylindrical pillars (radius $b = 1.2\ \mu$m and height $h = 6\ \mu$m), as a function of ϕ. The full and open symbols correspond to $\Omega = 10\ \mu$L and $\Omega = 20\ \mu$L, respectively.

brought in motion; the smaller ϕ, the smaller the tilting angle α (measured from the horizontal) at which the corresponding drop starts moving. We report in Figure 2 two series of measurements (for two water drop volumes), where the angle α is plotted as a function of ϕ, which is the mean pillar density below the drop.

For these millimetric drops, the angle α increases from 10 to 75° as ϕ goes from 5 to 30%. The adhesion of water drops increases (roughly) linearly with ϕ, that is, with the number of defects on which they can pin. At larger pillar densities, the drops remain pinned even on vertical samples. Figure 2 also shows that bigger drops (at a fixed ϕ) systematically (and logically) slide at smaller slopes. The increase of the hysteresis with the density of defects has been reported often,[15,17−20] in particular for solids decorated with chemical defects. In such situations, the pinning mainly occurs on defects, but also on the rest of the solid where a residual roughness coexists with uncontrolled chemical heterogeneities. Hence, the case of fakir drops for which pinning is limited to the sole pillars appears to be particularly ideal for a quantitative study of hysteresis.

Measuring the sliding angle α can give access to contact angle hysteresis. Since small drops are hardly deformed by gravity, they remain spherical (radius R) with a circular contact line of radius r, geometrically related to R by the relationship $r = R \sin \theta^*$, denoting θ^* as the mean contact angle below the drop. The angle θ^* is expected to be a function of the pillar density, as shown by the so-called Cassie model;[4,6] θ^* is an average between the Young contact angle on the solid ($\theta = 100°$ in our case) and the angle on air (180°), weighed by their respective proportion ϕ and $1 - \phi$, which yields $\cos \theta^* = -1 + \phi(1 + \cos \theta)$.

When a drop starts moving, its weight balances the force arising from contact hysteresis, which can be written as $\rho\Omega g \sin \alpha = \pi r \gamma\ \Delta\cos \theta$, denoting ρ and γ as the liquid density and surface tension.[21] Here we assumed that half the drop (the trailing edge) meets the solid with a receding angle θ_r while the other half (the leading edge) joins it with an advancing angle θ_a, which was shown to be a realistic approximation.[22] Hence, the value of the contact angle hysteresis $\Delta\cos \theta$ can be deduced from the measurement of α. We display the corresponding results in Figure 3, as a function of the pillar density ϕ.

The two series of data collapse on the same curve; we indeed expect that the value of the hysteresis does not depend on the drop volume. In the same figure, we added a few data (noted with cross symbols) obtained by measuring directly (i.e., optically) the angles θ_a and θ_r for water drops on various pillar densities. These data are found to be in good agreement with the other series. Figure 3 also shows that the variation of the

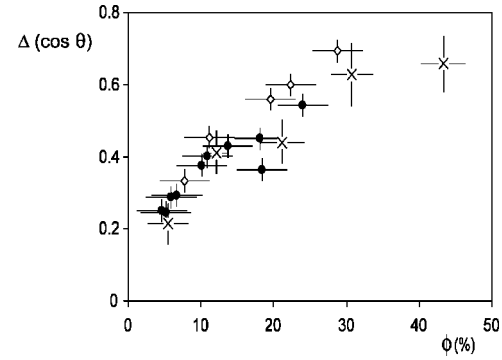

Figure 3. Contact angle hysteresis extracted from the data in Figure 2 (full and empty symbols from drop volumes $\Omega = 10\ \mu$L and $\Omega = 20\ \mu$L, respectively). The hysteresis $\Delta\cos \theta$ is defined as the difference between the cosines of the receding and advancing angles. In the same plot, we also display direct measurements of the hysteresis (marked with crosses), where advancing and receding angles are measured optically as slowly filling and emptying water drops. The hysteresis is observed to increase in a nonlinear fashion with the pillar density.

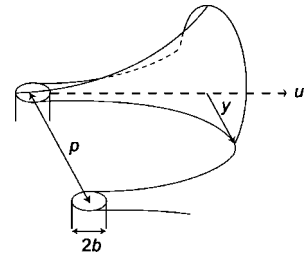

Figure 4. As we try to displace it (to the right in the figure), a fakir drop resists the motion by pinning at the edges of the defects on which it stands. The energy stored in this deformation fixes the amplitude of the hysteresis.

hysteresis is not linear in ϕ; this physically means that the effect of the number of pillars is not simply additive (as we could think naively). Besides, it is observed that even small pillar densities provide a significant residual contact angle hysteresis. We now interpret these different facts.

Calculating the hysteresis is generally a difficult (if not to say impossible) task. We need to understand quantitatively the way defects pin the line, and how these defects interact with each other. Even if knowing the precise map of the solid defects (either physical or chemical), there is generally no prediction for the quantity $\Delta\cos \theta$. Major exceptions to this statement are the classical models by Joanny and de Gennes[23] and by Pomeau and Vannimenus,[24] both published in the mideighties and complemented by Raphael and de Gennes.[25] These models assume dilute and strong defects, so that the line can efficiently pin on them. When trying to displace a liquid on such solids, the contact line largely deforms, as sketched in Figure 4. We assume that the hysteresis primarily comes from this resistance at the trailing edge of a drop. As a matter of fact, the leading edge in a fakir state shows very little resistance to motion, as noted by Gao and McCarthy,[26] and we neglect its contribution to the hysteresis.

As already pointed out, the force F per unit length required to move the line can be written:

$$F = \gamma \Delta\cos \theta \tag{1}$$

The energy $F\,\mathrm{d}x$ corresponding to a displacement of the line by a distance $\mathrm{d}x$ arises from pinning and depinning on the

dx/p^2 defects (per unit length) met by the line along its progression. Denoting ε as the energy per defect, we thus simply have

$$\gamma\Delta\cos\theta = \varepsilon/p^2 \quad (2)$$

We expect ε to depend on the shape of the defect; complex contours should generate a large ε and a large hysteresis, as reported experimentally by Öner and McCarthy.[27] Conversely, pinning and thus hysteresis will be minimized on defects either small or rounded, which is also in agreement with observations by Gao and McCarthy.[28] For cylindrical posts, ε might simply be a wetting energy proportional to the wetted area ($\varepsilon \approx \pi b^2\gamma$), which would immediately yield a hysteresis linear in ϕ ($\Delta\cos\theta \sim \phi$). This behavior is not observed in Figure 3, and we infer from the deformation sketched in Figure 4 that the energy stored in the deformation should also reflect the long liquid/vapor tails developing as one tries to displace the liquid.

For the sake of simplicity, we first assume an equilibrium (Young) angle of 90° and follow the approach proposed by Joanny and de Gennes.[23] The defects are the pillars' tops, that is, disks of radius b and mutual distance p with $b \ll p$, our hypothesis of dilute defects. As the contact line pins on the edge of a pillar as sketched in Figure 4, the tail of the drop forms a surface of zero curvature; the drop is very large at the scale of the defects, and it fixes the curvature at this (nearly) zero value. Hence the deformation of the line can be written: $y = b\cosh(u/b) \approx 1/2\ b\exp(u/b)$, which yields a maximum deformation u for $y \approx p/2$ given by

$$u \approx b\ln(p/b) \quad (3)$$

On the other hand, the force on each defect can be written

$$f \approx a\pi b\gamma \quad (4)$$

where a is a number depending on the detail of the line distortion; the larger this distortion, the larger a. By taking advantage of the slow logarithmic variation in eq 3, we deduce the force/deformation relationship:

$$f \approx a\pi\gamma u/\ln(p/b) \quad (5)$$

Force f and deformation u are proportional to each other! Equation 5 defines the behavior of a spring of stiffness $K = a\pi\gamma/\ln(p/b)$.[23] This stiffness is fixed by the liquid surface tension, a common feature when deforming a liquid/vapor interface. But it also contains a dimensionless parameter, which is a weak function of the geometrical characteristics of the defects. As seen in Figure 4, the solid/liquid surface area remains fixed as the liquid is distorted. The only energy stored in the deformation is the liquid/vapor surface energy, which yields: $\varepsilon = 1/2Ku^2$. Hence, we get

$$\varepsilon \approx 1/2a\pi b^2\gamma\ln(p/b) \quad (6)$$

Using eq 2 and the definition of ϕ ($\phi = \pi b^2/p^2$), we eventually find an expression for the contact angle hysteresis

$$\Delta\cos\theta \approx a/4\phi\ln(\pi/\phi) \quad (7)$$

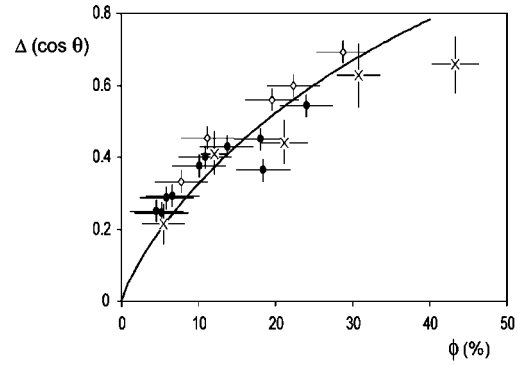

Figure 5. Comparison between the hysteresis measured on a superhydrophobic material (in the fakir state, on a density ϕ of pillars) and the hysteresis expected from eq 7. The data are the ones from Figure 3 (same symbols) and eq 7 is drawn with a full line (with $a = 3.8$).

This expression consists of two terms: the linear term in ϕ just reflects the additivity of defects; however, it is corrected by the logarithmic term, which originates from the shape of the distorted line and which is also sensitive to the defect density. $\Delta\cos\theta$ logically vanishes as the density of defects tends toward 0, but the slow divergence of the logarithm makes this variation quite pathologic; even very few defects are expected to generate an appreciable contact angle hysteresis.

We compare in Figure 5 the contact angle hysteresis measured in a fakir state to the one expected from eq 7 (drawn in full line), as a function of the defect density ϕ. It is observed that a function of the type $\phi|\ln\phi|$ nicely captures the data, reproducing both the residual hysteresis at small ϕ and the convexity of the curve. The numerical coefficient a deduced from the fit suggests a pinning force per pillar (eq 4): $f \approx 3.8\pi b\gamma$. A nave argument would let us expect a coefficient of the order of 2 (pinning proportional to the cylinder perimeter). However, any distortion of the line caused by irregularities at the edge or pinning on two pillars would immediately impact this factor and contribute to increase it. More importantly, the drop deformation in the fakir state (Figure 4) implies the formation of a liquid/vapor interface below each "tongue" of liquid, which contributes to increase the energy stored in the deformation.

We also notice that a point at large ϕ significantly deviates from the fit. The condition of dilute pillars is not satisfied anymore, and the model, which assumes that each defect distorts independently the line, should in this limit overestimate the hysteresis; then the line will take "short cuts" across the concentrated pillars. The critical density for which these collective effects need to be invoked here is 40%, significantly higher than the 10−20% reported in previous studies.[19,20] This might be related to our system, for which pinning only takes place on micropillars, while there is in more conventional systems an additional pinning on the solid between the defects, which modifies the actual defects density. The Joanny/de Gennes model thus seems be particularly relevant for understanding the characteristics of contact angle hysteresis in the fakir state. This state indeed fulfills the main assumptions of this model; the "defects" are dilute, well defined, and generate a strong pinning for the design we chose. In addition, the rest of the "substrate" is completely ideal; it consists of air, which does not provide any additional pinning of the line. The fakir state thus appears to be a model-system for the study of contact angle hysteresis, in particular in the limit of small defect densities, for which we generally cannot neglect the contribution of the rest of the (not-perfectly ideal) solid. It would be useful to extend this approach to other types of solid microtextures, in particular for under-

standing quantitatively the strong reduction of hysteresis (and thus of drop adhesion) observed for some particular designs.[28]

Acknowledgment. We dedicate this paper to the memory of P. G. de Gennes, who not only stimulated and constantly encouraged experiments around him, but also set in his laboratory at Collège de France a unique and unforgettable atmosphere of freedom and open-mindness.

References and Notes

(1) Onda, T.; Shibuichi, S.; Satoh, N.; Tsujii, K. *Langmuir* **1996**, *12*, 2125–2127.
(2) Gao, X. F.; Yan, X.; Yao, X; Xu, L.; Zhang, K.; et al. *Adv. Mater.* **2007**, *19*, 2213–2215.
(3) Ou, J.; Perot, B.; Rothstein, J. P. *Phys. Fluids* **2004**, *16*, 4635–4643.
(4) Quéré, D. *Annu. Rev. Mat. Res.* **2008**, *38*, 71–99.
(5) Wenzel, R. N. *Ind. Eng. Chem.* **1936**, *28*, 988–994.
(6) Cassie, A. B. D.; Baxter, S. *Trans. Faraday Soc.* **1944**, *40*, 546–551.
(7) Johnson, R. E.; Dettre, R. H. *Adv. Chem. Ser.* **1964**, *43*, 112–135.
(8) Lafuma, A.; Quéré, D. *Nat. Mat.* **2003**, *2*, 457–460.
(9) Yoshimitsu, Z.; Nakajima, A.; Watanabe, T.; Hashimoto, K. *Langmuir* **2002**, *18*, 5818–5822.
(10) Brandon, S.; Wachs, A; Marmur, A. *J. Colloid Interface Sci.* **1997**, *191*, 110–116.
(11) Extrand, C. W. *Langmuir* **2002**, *18*, 7991–7999.
(12) McHale, G.; Shirtcliffe, N. J.; Newton, M. I. *Langmuir* **2004**, *20*, 10146–10149.
(13) Kusumaatmaja, H.; Yeomans, J. M. *Langmuir* **2007**, *23*, 6019–6032.
(14) De Simone, A.; Grunewald, N.; Otto, F. *Networks Heterog. Media* **2007**, *2*, 211–225.
(15) Rolley, E.; Guthmann, C. *Phys. Rev. Lett.* **2007**, *98*, 166105.
(16) Callies, M.; Chen, Y.; Marty, F.; Pépin, A.; Quéré, D. *Microelectron. Eng.* **2005**, *78*−*79*, 100–105.
(17) Di Meglio, J. M.; Quéré, D. *Europhys. Lett.* **1990**, *11*, 163–168.
(18) Di Meglio, J. M. *Europhys. Lett.* **1992**, *17*, 607–612.
(19) Ramos, S. M. M.; Charlaix, E.; Benyagoub, A.; Toulemonde, M. *Phys. Rev. E* **2003**, *67*, 031604.
(20) Ramos, S.; Tanguy, A. *Eur. Phys. J. E* **2006**, *19*, 433–440.
(21) Furmidge, C. G. L. *J. Colloid. Sci.* **1962**, *17*, 309–314.
(22) Quéré, D.; Azzopardi, M. J.; Delattre, L. *Langmuir* **1998**, *14*, 2213–2216.
(23) Joanny, J. F.; de Gennes, P. G. *J. Chem. Phys.* **1984**, *81*, 552–562.
(24) Pomeau, Y.; Vannimenus, J. *J. Colloid Interface Sci.* **1985**, *104*, 477–488.
(25) Raphael, E.; de Gennes, P. G. *J. Chem. Phys.* **1989**, *90*, 7577–7584.
(26) Gao, L. C.; McCarthy, T. J. *Langmuir* **2006**, *22*, 6234–6237.
(27) Öner, D.; McCarthy, T. J. *Langmuir* **2000**, *16*, 7777–7782.
(28) Gao, L.; McCarthy, T. J. *J. Am. Chem. Soc.* **2006**, *128*, 9052–9053.
JP8066876